

UC Santa Barbara

UC Santa Barbara Previously Published Works

Title

A Modular, DNA-Based Beacon for Single-Step Fluorescence Detection of Antibodies and Other Proteins

Permalink

<https://escholarship.org/uc/item/36s5r9xv>

Journal

Angewandte Chemie International Edition, 54(45)

ISSN

1433-7851

Authors

Ranallo, Simona
Rossetti, Marianna
Plaxco, Kevin W
et al.

Publication Date

2015-11-02

DOI

10.1002/anie.201505179

Peer reviewed



HHS Public Access

Author manuscript

Angew Chem Int Ed Engl. Author manuscript; available in PMC 2016 November 02.

Published in final edited form as:

Angew Chem Int Ed Engl. 2015 November 2; 54(45): 13214–13218. doi:10.1002/anie.201505179.

A modular, DNA-based “beacon” for the single-step fluorescent measurement of antibodies and other proteins**

Simona Ranallo,

Dipartimento di Scienze e Tecnologie Chimiche, University of Rome Tor Vergata, Via della Ricerca Scientifica, Rome 00133, (Italy)

Marianna Rossetti,

Dipartimento di Scienze e Tecnologie Chimiche, University of Rome Tor Vergata, Via della Ricerca Scientifica, Rome 00133, (Italy)

Prof. Kevin W. Plaxco,

Center for Bioengineering & Department of Chemistry and Biochemistry, University of California, Santa Barbara, California 93106, United States

Prof. Alexis Vallée-Bélisle, and

Laboratory of Biosensors & Nanomachines, Département de Chimie; Université de Montréal; C.P. 6128, Succursale Centre-ville, Montréal, Québec H3C 3J7, Canada

Prof. Francesco Ricci

Dipartimento di Scienze e Tecnologie Chimiche, University of Rome Tor Vergata, Via della Ricerca Scientifica, Rome 00133, (Italy)

Alexis Vallée-Bélisle: a.vallee-belisle@umontreal.ca; Francesco Ricci: francesco.ricci@uniroma2.it

Abstract

Here we demonstrate a versatile platform for the one-step fluorescent detection of both monovalent and multivalent proteins. Specifically, we have designed a conformational-switching, stem-loop DNA scaffold that presents a small molecule, polypeptide or nucleic-acid (e.g., aptamer, transcription factor binding site) recognition element on each of its two stem strands. The steric strain associated with the binding of one (multivalent) or two (monovalent) target molecules to these elements opens the stem, enhancing the emission of an attached fluorophore/quencher pair. The sensors are rapid (<10 minutes) and selective, supporting the ready detection of specific proteins even in complex samples, such as blood serum. The platform is also versatile: using it we have measured five bivalent proteins (four antibodies and the chemokine platelet-derived growth factor) and two monovalent proteins (a Fab fragment and the transcription factor TBP) all with low nanomolar detection limits and no detectable cross-reactivity.

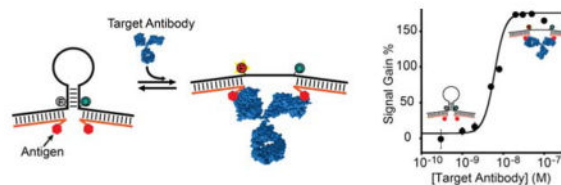
** This work was supported by the European Research Council, ERC (project no. 336493) (FR), by the Natural Sciences and Engineering Research Council of Canada (NSERC) through Grant No. 2014-06403 (AVB) and by the National Institutes of Health through Grant No. AI107936 (KWP).

Correspondence to: Francesco Ricci, francesco.ricci@uniroma2.it.

Experimental Section

Experimental details in supporting information.

Graphical Abstract



Keywords

DNA nanotechnology; Molecular devices; Antibodies; Aptamers

Recent years have seen significant increase in the number of well-characterized biomarkers, proteins present in blood or on cells that are diagnostic of disease.^[1–3] Unfortunately, however, current methods for the detection of such markers are either multistep, wash- and reagent-intensive processes requiring sophisticated, laboratory-bound measurement protocols (e.g., ELISA or Western Blot assays) or are at best only semi-quantitative (e.g., immunochemical dipsticks).^[4–6] These drawbacks limit accessibility to quantitative molecular diagnostics, resulting in delayed treatment, reduced compliance and poorer outcomes.^[1,2,7] In contrast to the cumbersome, multistep nature of current detection schemes, however, the biomolecular receptors present in organisms respond to changes in the concentration of their targets quantitatively and without needing reagent additions or wash steps.^[8,9] Indeed, these receptors detect thousands of distinct molecules in real time even in the complex, in vivo environment.^[10] Building artificial biosystems of similar simplicity, convenience and selectivity represents a major bioengineering goal.

Among the different strategies used by naturally occurring “sensors”^[11] is conformational-switching. In this a receptor undergoes a large-scale, binding-induced conformational change in the presence of its target.^[8,9] Because their signalling is linked to a specific, binding-induced event, such “switches” are highly selective, and support detection even in highly complex sample matrices.^[10] Moreover, such conformational changes can also be harnessed in artificial systems, where they can be used to generate an optical or electrochemical signal without the addition of exogenous reagents or coupling to exogenous biochemical reactions.^[12,13] Motivated by these considerations we have developed a single-step method for the quantitative measurement of specific proteins that is rapid, inexpensive and highly selective. To do this we took inspiration from DNA molecular beacons, synthetic nucleic acid switches for the detection of specific DNA or RNA sequences and now widely used for the detection of specific oligonucleotides^[14] and newer, FRET- and electrochemical methods for the detection of specific antibodies.^[12,15,16]

Molecular beacons are conformation-changing DNA-based nanoswitches modified with a fluorophore/quencher pair. In the absence of target they adopt a stem-loop conformation that, upon hybridization to their target, opens, segregating the reporters and enhancing fluorescence. To create nanoswitches that respond instead to protein targets we designed a beacon with single-stranded tails appended to each end (Figure 1, left). This allows us to add recognition elements (hexagons in Figure 1) that specifically bind the protein of interest via

their conjugation to the appropriate DNA or PNA strand (red strands in Figure 1). Given this structure, the binding of one copy of a bivalent protein (e.g., an antibody) or two copies of a monovalent protein opens the stem, enhancing fluorescence (Figure 1, right).

As a test bed for the optimization of our sensors we first developed a sensor for antibodies binding digoxigenin (Dig) (Figure 2A, left). To create this we hybridized Dig-modified DNA strands to the tailed stem-loop scaffold. The performance of such switches is a function of the stability of their stem.^[17] Specifically, an unstable stem opens partially even in the absence of target, thus potentially reducing signal gain. In contrast, an overly stabilized stem reduces affinity (because binding must overcome a higher barrier). To optimize sensor performance we thus characterized variants (Figure 2B) differing in stem stability and loop length (Figure 2C). Melting curves performed in the absence and presence of saturating target (Figure 2D, S1) suggest that a five base pair, 3 GC stem with a 15-base poly-T loop (variant #4) produce good performance (e.g., 150% gain at saturating target) at the 25–35°C temperatures of interest for clinical applications (Figure 2E). Simulations (Nupack)^[18] suggest that this construct is stable enough that, in the absence of target, 98% of the unbound switches are in their non-emissive, stem-loop configuration, maximizing gain without unnecessarily reducing affinity.

The optimized sensor achieves low-nanomolar detection limits (Figure 2F). Of note, the sensor's binding curve appears bilinear rather than hyperbolic (i.e., rather than a Langmuir isotherm). This suggests that we are in the “ligand-depletion” (or “tight-binding”) regime.^[19] That is, the effective affinity (K_D) for the target is well below the 10 nM switch concentration, and thus each new aliquot of antibody added binds to near completion until all of the switches are occupied. Consistent with this, the target concentration at which the observed signal change is half the maximum signal change ($K_{1/2}$) is, at 4.9 ± 2.4 nM, within error of the 5 nM (one half of 10 nM) value expected for a stoichiometric 1:1 target-to-sensor ratio. Further confirming this, binding curves collected over a range of sensor concentrations (Figure S2) always produce $K_{1/2}$ within error of the value expected for a 1:1 stoichiometry (Figure 2G).

The modular nature of our approach renders it easily expandable to the measurement of new proteins via the expedient of changing its recognition elements (Figure 1). To demonstrate this we first used recognition elements specific for three monoclonal antibodies: the small molecule dinitrophenol (DNP),^[20] the 8-residue FLAG peptide,^[21] and a 13-residue peptide from HIV-1 p17 matrix protein.^[13d,e] We employed peptide nucleic acid (PNA) rather than DNA strands for the latter two receptors as the synthesis of PNA-peptide chimeras is particularly facile. The stabilities of all three modified stem-loops are comparable (Figure S3) and optimal signalling is achieved when using switch variant #4 (Figure S4). Consistent with this, all three sensors respond to their specific targets at low nanomolar concentrations, with all three $K_{1/2}$ falling within error of 5 nM (again suggesting that we are in a ligand-depletion regime^[19] as the effective affinity of these IgG antibodies is in the low nanomolar regime^[22]). All three likewise exhibit similar signal gains (120–150%), suggesting that the construct optimized for the detection of anti-Dig antibodies also performs well for the detection of these antibodies. All three appear specific for their target, with none of the three exhibit any significant cross-reactivity with the targets of the others (Figure 3A–C).

Focusing in on the sensor targeting anti-p17 antibodies (a biomarker for the detection of HIV infection,^[1,13e] we find that the sensor is also rapid, achieving 90% of the maximum signal after just 2 minutes (Figure S5, left).

The binding-induced conformational change that underlies their signalling renders our sensors selective enough to deploy in complex samples. Our anti-p17 antibody sensor, for example, performs well when deployed in 90% blood serum, producing a $K_{1/2}$ within error of that obtained in simple buffer (Figure S5, right). As expected, however, the gain observed under these circumstances is lower due to the higher background fluorescence of this sample matrix. The other three antibody-detecting sensors also exhibit good performance under these historically challenging conditions (Figure S6).

Our platform is generalizable to the detection of other (i.e., non-antibody) bivalent proteins. To show this we fabricated a sensor displaying two copies of a 35-base aptamer binding the dimeric protein platelet-derived growth factor (PDGF) with a reported sub-nanomolar affinity.^[23] This sensor recognizes its target with a $K_{1/2}$ of 4.6 ± 2.5 nM, again indicating a 1-to-1 binding stoichiometry (Figure 3D). Of note, at molecular weight of ca. 10 kDa the aptamer recognition element used in this construct is quite larger, which speaks to the versatility of our approach. This said, however, this sensor's 30% gain is rather less than that of our antibody-recognizing sensors. We presume this occurs due to one or more of the following: 1) a difference in binding geometry, 2) that the rather large recognition element leads to partial stem opening in the absence of its target (as demonstrated by melting curves: Figure S8), and/or 3) because PDGF is smaller than an antibody, and thus may not lead to as great a separation between the quencher and fluorophore.

Although we initially intended our sensors to detect bivalent proteins, such as antibodies, we demonstrate here that it can nevertheless be used for the detection of monovalent targets if the binding of two copies of the target produces enough steric hindrance to open the stem. To demonstrate this we built sensors targeting a Dig-binding Fab fragment and the transcription factor TATA binding protein (TBP), the latter of which is recognized by a 20-base, double-stranded hairpin.^[13a-b,24] Both sensors respond robustly to their specific targets, albeit with lower gain than that of sensors detecting bivalent targets (Figure 4, S9). The Fab-detecting sensor appears to be operating close to the ligand-depletion regime as the 20 ± 4 nM $K_{1/2}$ is reasonably close to the 10 nM expected for a 1:2 stoichiometric ratio; binding curves collected over a range of sensor concentrations provide further support for this claim (Figure S10). The 114 ± 5 nM $K_{1/2}$ of the TBP sensor, in contrast, is far higher than that which would be expected were we in the ligand-depletion regime, which is surprising given the 2 nM intrinsic affinity of TBP for its consensus sequence.^[24] This presumably arises due to steric effects reducing the affinity of the protein for its recognition element in these constructs.

The versatility and modular nature of our sensors renders it easy to convert them into molecular AND-logic gates^[25] that signal the concomitant presence of two different macromolecular targets. To demonstrate this we fabricated a single sensor presenting both Dig and DNP (Figure 5, top). The addition of either anti-Dig or anti-DNP antibodies in

isolation does not lead to an increase in fluorescence (Figure 5, bottom). As expected, however, activation is observed in the simultaneous presence of both antibodies.

Taking inspiration from naturally occurring receptors, which often signal the presence of their molecular target via binding-induced conformational changes, we have developed a new generalizable, highly versatile sensing platform for the one-step detection of monovalent and multivalent macromolecular targets. More specifically, we have rationally designed a conformational-switching, optically signaling stem-loop DNA that supports the introduction of two copies of any of a wide range of polypeptide, small molecule, or oligonucleotide recognition elements. The binding of one (multivalent) or two (monovalent) target molecules to these recognition elements opens the stem, producing a fluorescence signal monotonically related to the target's concentration. This novel DNA nanoswitch can, in principle, be adapted to the detection of any macromolecular target for which a recognition element can be attached to a DNA or PNA anchoring strand. In support of this claim, we have used our platform to measure the concentrations of five bivalent targets (including four antibodies) and two monovalent protein targets. We detect all seven targets sensitively (at low nanomolar levels) and with excellent specificity (we observe no significant cross reactivity). Finally, the nanoswitches are rapid (less than 10 min) and, due to the robustness of their structure-switching signaling mechanism, perform well in complex samples matrices, such as blood serum.

Given these attributes our modular nanoswitches may be advantageous over existing methods for the detection of specific macromolecules. For example, although the lack of any amplification step likely renders our platform less sensitive than ELISAs or methods that use binding-induced conformational changes to modulate enzyme activity^[13e,26], the reagentless, binding-induced signaling mechanism underlying our sensors drastically simplifies detection by eliminating washing steps and reagent additions and by reducing sensitivity to temperature and other environmental factors that alter catalysis. Our platform's performance also compares well with other recently developed, similarly homogeneous assays^[15,16,26–28] (and reviewed in 13d). Our switch-based approach could nevertheless benefit from further improvements. Its limited dynamic range, for example, could be further extended,^[29] and the introduction of FRET-based reporters would support ratiometric measurements that can control for instrumental and sample-to-sample variations.^[30] Irrespective, we believe that the modularity and convenience of our platform suggests it may be of utility in a range of applications, including point-of-care diagnostics and in-vivo imaging.^[10]

Supplementary Material

Refer to Web version on PubMed Central for supplementary material.

References

1. Yager P, Domingo GJ, Gerdes J. *J Annu Rev Biomed Eng.* 2008; 10:107–144.
2. Yetisen AK, Akram MS, Lowe CR. *Lab Chip.* 2013; 13:2210–2251. [PubMed: 23652632]
3. Fu E, Yager P, Floriano PN, Christodoulides N, McDevitt JT. *IEEE Pulse.* 2011; 2:40–50. [PubMed: 22147068]

4. Shen J, Li Y, Gu H, Xia F, Zuo X. *Chem Rev.* 2014; 114:7631–7677. [PubMed: 25115973]
5. Ríos A, Zougagh M, Avilaa M. *Anal Chim Acta.* 2012; 740:1–11. [PubMed: 22840644]
6. Ornberg RL, Harper TF, Liu H. *Nat Methods.* 2005; 2:79–81.
7. (a) Martinez AW, Phillips ST, Whitesides GM, Carrilho E. *Anal Chem.* 2010; 82:3–10. [PubMed: 20000334] (b) Park IS, Eom K, Son J, Chang WJ, Park K, Kwon T, Yoon DS, Bashir R, Lee SW. *ACS Nano.* 2012; 6:8665–8873. [PubMed: 22967242] (c) Stern E, Vacic A, Rajan NK, Criscione JM, Park J, Ilic BR, Mooney DJ, Reed MA, Fahmy TM. *Nat Nanotechnol.* 2010; 5:138–142. [PubMed: 20010825] (d) Lee WG, Kim YG, Chung BG, Demirci U, Khademhosseini A. *Adv Drug Deliver Rev.* 2010; 62:449–457.
8. Zhang H, Li F, Dever B, Li XF, Le XC. *Chem Rev.* 2013; 113:2812–2841. [PubMed: 23231477]
9. Wu AH. *Clin Chim Acta.* 2006; 369:119–124. [PubMed: 16701599]
10. (a) Plaxco KW, Soh HT. *Trends Biotechnol.* 2011; 29:1–5. [PubMed: 21106266] (b) Vallée-Bélisle A, Plaxco KW. *Curr Opin Struct Biol.* 2010; 20:518–526. [PubMed: 20627702] (c) Ha JH, Loh SN. *Chem Eur J.* 2012; 18:7984–7999. [PubMed: 22688954]
11. (a) Inci F, Tokel O, Wang S, Gurkan UA, Tasoglu S, Kuritzkes DR, Demirci U. *ACS Nano.* 2013; 7:4733–4745. [PubMed: 23688050] (b) Stratton MM, Loh SN. *Protein Sci.* 2011; 20:19–29. [PubMed: 21064163] (c) Laczka O, Ferraz RM, Ferrer-Miralles N, Villaverde A, Munoz FX, Del Campo FJ. *Anal Chim Acta.* 2009; 641:1–6. [PubMed: 19393360] (d) Walt DR. *ACS Nano.* 2009; 3:2876–2880. [PubMed: 19856977]
12. Vallée-Bélisle A, Ricci F, Uzawa T, Xia F, Plaxco KW. *J Am Chem Soc.* 2012; 134:15197–15200. [PubMed: 22913425]
13. (a) Vallée-Bélisle A, Bonham AJ, Reich NO, Ricci F, Plaxco KW. *J Am Chem Soc.* 2011; 133:13836–13839. [PubMed: 21815647] (b) Bonham AJ, Hsieh K, Ferguson BS, Vallée-Bélisle A, Ricci F, Soh HT, Plaxco KW. *J Am Chem Soc.* 2012; 134:3346–3348. [PubMed: 22313286] (c) Merckx M, Golynskiy MW, Lindenburg LH, Vinkenburg JL. *Biochemical Soc T.* 2013; 41:1201–1205. (d) Banala S, Arts R, Aper SJA, Merckx MM. *Org Biomol Chem.* 2013; 11:7642–7649. [PubMed: 24091607] (e) Banala S, Aper SJA, Schalk W, Merckx M. *ACS Chem Biol.* 2013; 8:2127–2132. [PubMed: 23941162]
14. (a) Tyagi S, Kramer FR. *Nat Biotechnol.* 1996; 14:303–308. [PubMed: 9630890] (b) Marras SAE, Tyagi S, Kramer FR. *Clin Chim Acta.* 2006; 363:48–60. [PubMed: 16111667]
15. Golynskiy MV, Rurup WF, Merckx M. *ChemBioChem.* 2010; 11:2264–2267. [PubMed: 20928879]
16. Cash KJ, Ricci F, Plaxco KW. *Chem Commun.* 2009:6222–6224.
17. Vallée-Bélisle A, Ricci F, Plaxco KW. *Proc Natl Acad Sci USA.* 2009; 106:13802–13807. [PubMed: 19666496]
18. Zadeh JN, Steenberg CD, Bois JS, Wolfe BR, Pierce MB, Khan AR, Dirks RM, Pierce NA. *J Comput Chem.* 2011; 32:170–173. [PubMed: 20645303]
19. Esteban Fernández de Ávila B, Watkins HM, Pingarrón KW, Plaxco JM, Palleschi G, Ricci F. *Anal Chem.* 2013; 85:6593–6597. [PubMed: 23713910]
20. Eshhar Z, Ofarim M, Waks TJ. *Immunol.* 1980; 124:775–780.
21. White RJ, Kallewaard HM, Hsieh W, Patterson AS, Kasehagen JB, Cash KJ, Uzawa T, Soh HT, Plaxco KW. *Anal Chem.* 2012; 84:1098–1103. [PubMed: 22145706]
22. (a) Jung HS, Yang T, Lasagna MD, Shi JJ, Reinhart GD, Cremer PS. *Biophys J.* 2008; 94:3094–3103. [PubMed: 18199665] (b) Wegner GJ, Lee HJ, Corn RM. *Anal Chem.* 2002; 74:5161–5168. [PubMed: 12403566]
23. (a) Lai RY, Plaxco KW, Heeger AJ. *Anal Chem.* 2007; 79:229–233. [PubMed: 17194144] (b) Cho M, Xiao Y, Nie J, Stewart R, Csordas A, Csordas AT, Oh SS, Thomson JA, Soh HT. *Proc Natl Acad Sci U S A.* 2010; 107:15373–15378. [PubMed: 20705898]
24. Nikolov DB, Chen H, Halay ED, Hoffman A, Roeder RG, Burley SK. *Proc Natl Acad Sci USA.* 1996; 93:4862–4867. [PubMed: 8643494]
25. Janssen BMG, Van Rosmalen M, Van Beek L, Merckx M. *Angew Chem Int Ed.* 2015; 54:2530–253.
26. (a) Geddie ML, Matsumura I. *J Mol Biol.* 2007; 369:1052–1059. [PubMed: 17467736] (b) de las Heras R, Fry SR, Li J, Arel E, Kachab EH, Hazell SL, Huang CY. *Biochem Biophys Res*

- Commun. 2008; 370:164–168. [PubMed: 18358235] (c) Ohmuro-Matsuyama Y, Chung CI, Ueda H. BMC Biotechnol. 2013; 13:31. [PubMed: 23536995] (d) Legendre D, Soumillion P, Fastrez J. Nat Biotechnol. 1999; 17:67–72. [PubMed: 9920272]
27. Tian L, Heyduk T. Anal Chem. 2009; 81:5218–5225. [PubMed: 19563210]
28. Oh KJ, Cash KJ, Lubin AA, Plaxco KW. Chem Commun. 2007; 46:4869–4871.
29. Vallée-Bélisle A, Ricci F, Plaxco KW. J Am Chem Soc. 2012; 134:2876–2879. [PubMed: 22239688]
30. Jares-Erijman EA, Jovin TM. Nature Biotechnol. 2003; 21:1387–1395. [PubMed: 14595367]

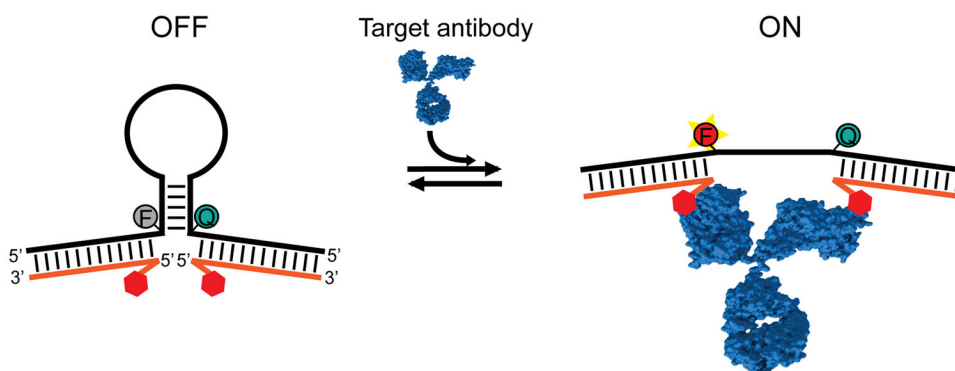
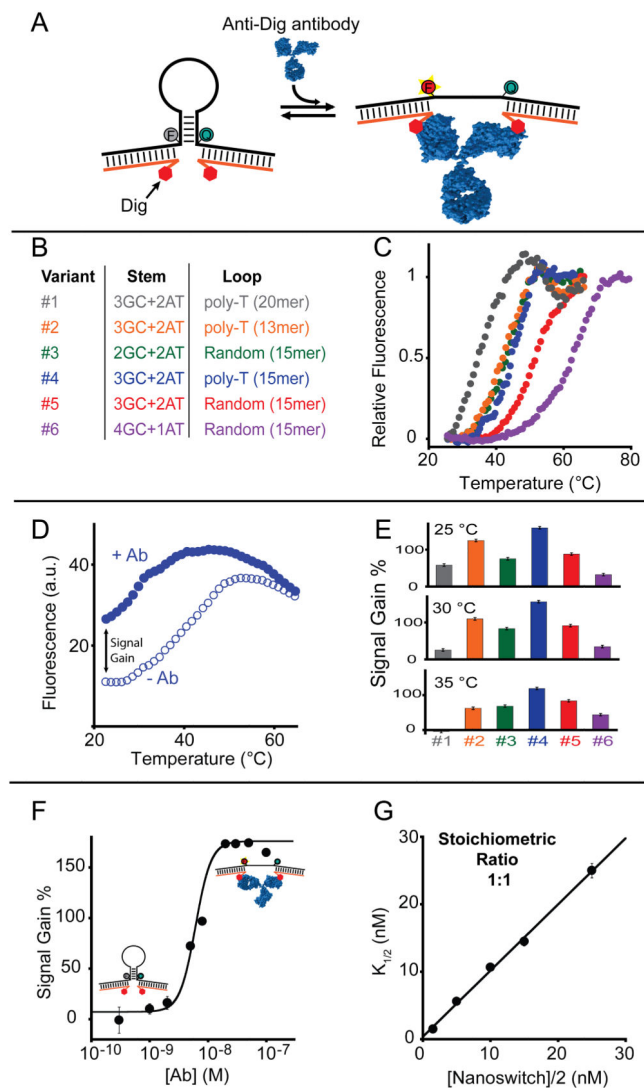


Figure 1.

Our protein-targeting sensor is composed of a fluorophore/quencher-modified DNA stem-loop containing two single-stranded tails. To create a target-responsive sensor, these tails are hybridized with DNAs conjugated to the appropriate recognition element (red hexagons). A frame inversion at one tail-stem junction ensures that the two tails meet “head-to-head” (3'-end-to-3'-end), thus allowing a single recognition-element modified strand sequence to populate both recognition sites. The binding of a bivalent macromolecule (here an antibody) to the two recognition elements opens the stem, allowing for rapid and sensitive protein detection. As shown later, the binding of two copies of a target is also sufficient to cause stem opening, allowing for the design of switches that respond to monovalent targets.

**Figure 2.**

(A) As proof-of-principle we employed digoxigenin (Dig) as a recognition element for the detection of anti-Dig antibodies. (B) We initially tested sensors varying in stem stability due to variations in stem GC content (2, 3 and 4 GC) and/or loop length (13 to 20 bases). (C) Melting curves obtained in the absence of the target illustrate their varying stabilities. (D) Comparison with curves obtained at 100 nM target (one is shown) provides a means of measuring the gain of each variant as a function of temperature. (Under these conditions antibody binding is effectively temperature independent; Figure S7.) (E) Sensors of intermediate stability exhibit the best compromise between gain and affinity, with a 3GC stem and a 15-base poly-T loop (variant #4) proving optimal. (F) The optimal sensor detects anti-Dig antibodies at low nanomolar concentrations. (G) $K_{1/2}$ changes with varying sensors' concentration in precisely the manner expected for a 1:1 binding stoichiometry, thus supporting the proposed sensing principle. The experiments shown here and in the following figures represent averages of three measurements; error bars reflect standard deviations. The binding and melting curves here and in the following figures were

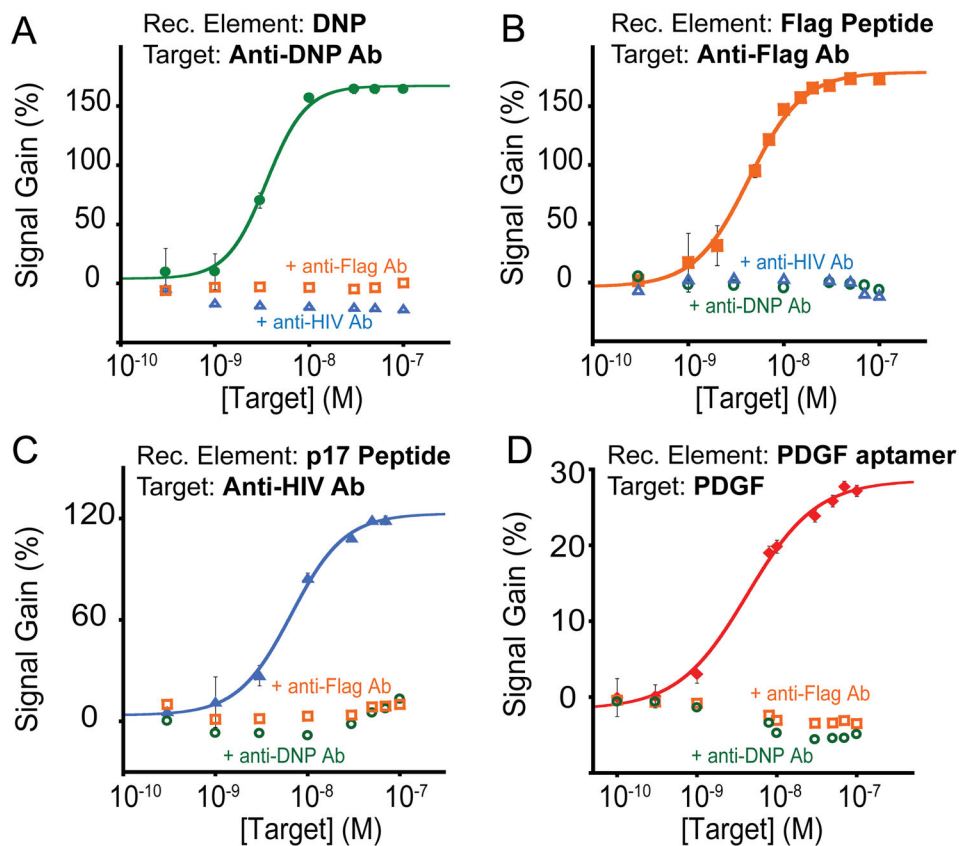
performed in 50 mM Na₂HPO₄, 150 mM NaCl, pH 7.0, with the nanoswitch at 10 nM unless otherwise noted.

Author Manuscript

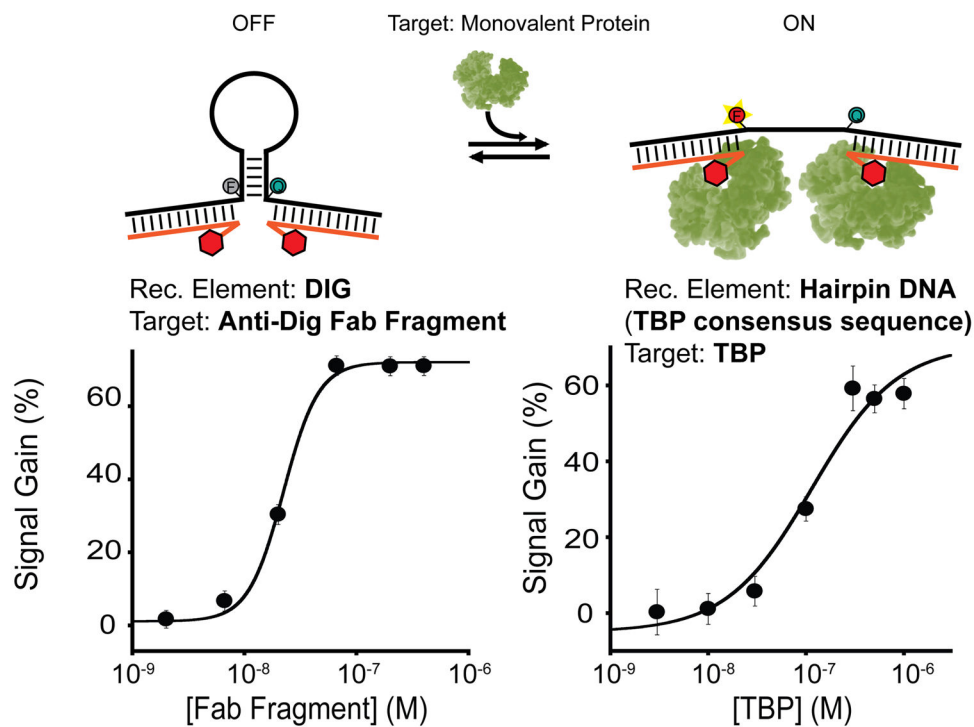
Author Manuscript

Author Manuscript

Author Manuscript

**Figure 3.**

Our modular platform is versatile and can easily be adapted to the detection of new targets via the expedient of changing the recognition element employed. Here we demonstrate this by using three different antigens recognized by specific antibodies: (A) dinitrophenol (DNP), (B) the 8-residue FLAG peptide, and (C) a 13-residue epitope excised from the HIV protein p17. (D) Using a 35-base aptamer as recognition element the platform can also be used to detect the bivalent chemokine PDGF. All four sensors respond to their specific target at low nanomolar concentrations whilst exhibiting no significant response to high concentrations of the other switches' targets

**Figure 4.**

(Top) Our platform can be also used for the detection of monovalent targets. In this case the signal change arises because the simultaneous binding of two copies of the target causes steric hindrance, opening the stem. Shown are sensors detecting a monovalent anti-Dig Fab fragment (bottom left) and the monovalent DNA-binding transcription factor TBP (bottom right). Both sensors readily detect their specific target at nanomolar concentrations.

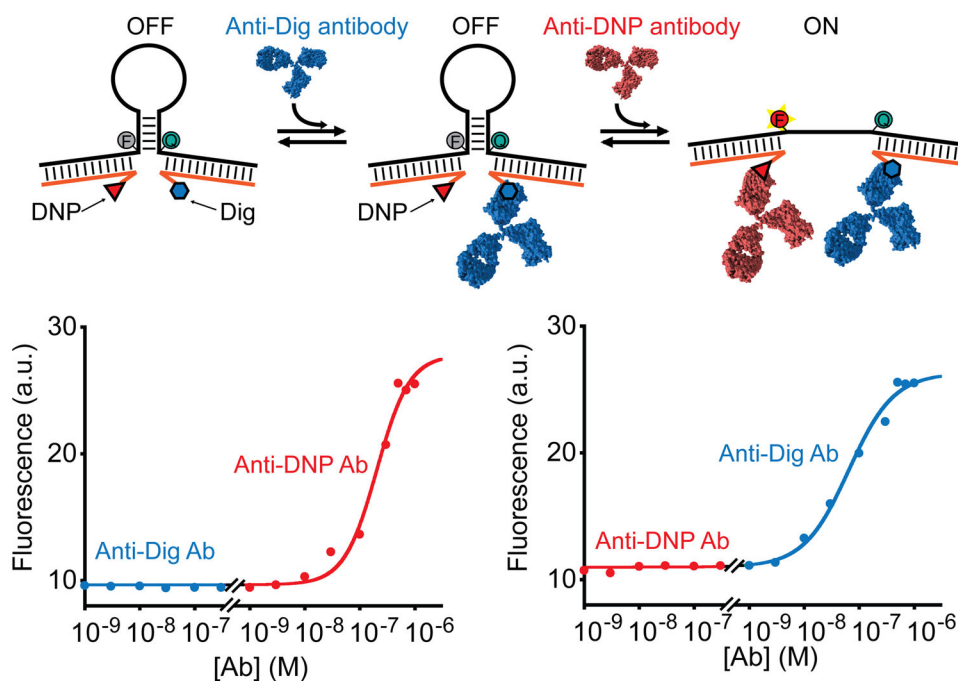


Figure 5. Modular sensors can serve as a molecular AND-logic gate that signals only in the simultaneous presence of two different macromolecular targets. (Top) To demonstrate this we modified a sensor with the recognition elements Dig and DNP. (Bottom) Only in the simultaneous presence of both anti-Dig and anti-DNP antibodies we observe any significant signal increase.